Determinants of Geographic Patterns in Seed Dispersal Modes in Continental U.S. Plant Communities

By

Shiqi Zheng

Advisor: Dr. James Clark

April 24, 2025

Duke | NICHOLAS SCHOOL *of* *the* ENVIRONMENT

Executive Summary

Seed dispersal is a critical ecological process that influences plant community structure, promotes regeneration, and determines species' abilities to track shifting climatic conditions. As climate change accelerates, understanding what drives variation in dispersal strategies is increasingly important for predicting biodiversity responses and informing conservation strategies. While broad patterns of dispersal modes—such as the dominance of animal-dispersed (zoochorous) plants in tropical forests and wind-dispersed (anemochorous) plants in higher latitudes—are well documented, these patterns have been less studied in temperate regions. Moreover, little is known about how dispersal modes covary with other plant functional traits and how their distribution is shaped by both abiotic conditions and biotic dispersal agents like animals.

This study addresses key knowledge gaps by evaluating the biogeographic and environmental structuring of plant dispersal modes across temperate and boreal forests in the continental United States. Specifically, it investigates:

1) Whether dispersal mode distributions vary predictably with climate, topography, and disperser availability;
2) Whether these patterns support the resource-availability hypothesis (which links dispersal strategies to environmental resource gradients) or the disperser-availability hypothesis (which links them to the abundance of dispersal agents); and
3) How dispersal modes are integrated with broader suites of plant functional traits.

To answer these questions, I applied a Predictive Trait Model (PTM) using the Generalized Joint Attribute Modeling (GJAM) framework. This Bayesian multivariate model jointly estimates how dispersal modes respond to environmental and biotic variables, including annual precipitation, temperature, wind speed, topographic position index (TPI), and a novel metric of disperser availability. Disperser demand was estimated by integrating species-level diet fractions, body mass, and density data for frugivorous birds and granivorous mammals using distance sampling from NEON data. Trait and plot data were obtained from a continental-scale forest inventory database (Qiu et al., 2022). Visualizations included distribution maps, climate space plots, model coefficient plots, and a dendrogram of trait responses.

Key Findings:
1) Geographic Trends: Zoochory is more common in warm, humid, low-latitude forests, while anemochory dominates in cooler, drier, and more open habitats in higher latitudes and elevations. This spatial partitioning aligns with expectations from tropical ecosystems.
2) Climatic Associations: In environmental space, zoochory is concentrated in areas of low water deficit and high temperature, whereas anemochory prevails in cooler and more water-limited conditions. These patterns suggest that environmental constraints shape dispersal mode prevalence across regions.
3) PTM Results: Despite directional associations, none of the environmental predictors had statistically significant effects. For zoochory, wind speed showed a negative association, while for anemochory, temperature and wind speed had weakly positive effects. Disperser demand showed little influence, possibly due to limitations in the input dataset.
4) Trait-Derived Clusters: A dendrogram of predictor effects showed that dispersal modes cluster with relevant traits—zoochory with fleshy fruits and broad leaves; anemochory

with winged fruits and needle-like foliage—highlighting their integration into broader ecological syndromes.

5) Species-Level Patterns: While plant height and seed mass were poor predictors of wind response, taxonomic patterns emerged. For example, Acer species consistently showed positive wind speed effects (some significant), reflecting adaptations for wind dispersal via samaras. Conversely, some conifers (e.g., Pinus sabiniana) had unexpectedly negative or variable responses.

Together, these findings highlight that while plant dispersal modes are clearly structured across geographic and climatic gradients, their underlying drivers are multifaceted and context-dependent. The co-occurrence of dispersal strategies with specific leaf, fruit, and seed traits suggests that dispersal is part of broader ecological syndromes shaped by environmental filtering. However, the limited predictive power of individual environmental variables underscores the challenges of modeling dispersal using coarse-scale data. This study also reveals important methodological limitations, including simplifications in the disperser demand metric, assumptions inherent in distance sampling, and spatial mismatches between plot-level and animal survey data. Moreover, the exclusion of multi-vector dispersal and long-distance dispersal events may overlook critical processes influencing range shifts. Future research should focus on improving the temporal and spatial resolution of both wind and animal data, incorporating more detailed dispersal traits (e.g., seed release height, aerodynamic morphology), and expanding taxonomic and functional coverage of dispersers. By integrating these improvements, future models can move toward more mechanistic, trait-based predictions of plant movement and community assembly under global change.

Introduction

Seed dispersal is an important life-history stage that determines the spatial distribution of plant offspring and underlies species' abilities to colonize new environments, escape unfavorable conditions, and respond to climate change (Janzen, 1970; Connell, 1971; Howe & Smallwood, 1982; Clark et al., 1998; Nathan & Muller-Landau, 2000). Most plants rely on passive dispersal by abiotic vectors (e.g., gravity, wind, water) or mutualistic interactions with animals (e.g., frugivores, scatter-hoarders). These dispersal modes have been tightly linked to fruit and seed morphology, suggesting a strong evolutionary interplay between dispersal vectors and plant functional traits (Willson et al., 1989). However, we still lack a clear understanding of how dispersal modes relate to other plant functional traits, and how dispersal modes are structured geographically and environmentally, particularly in temperate systems. Investigating drivers behind spatial patterns of seed dispersal modes is essential for predicting plant migration and range shifts under climate change. Without this knowledge, we can't make accurate projections of species range shifts.

Previous studies have documented broad geographic patterns in dispersal modes. For instance, zoochory (animal-dispersed seeds) dominates in tropical forests with high precipitation and vertebrate frugivore diversity (Chen et al., 2017; Almeida-Neto et al., 2008), whereas anemochory (wind-dispersed seeds) becomes more prevalent at higher latitudes and in drier, open habitats (Moles et al., 2007). In Amazonia, Correa et al. (2023) showed that dispersal mode frequencies are associated with both disperser availability and environmental conditions, highlighting two complementary hypotheses: the disperser-availability hypothesis, which suggests that the prevalence of dispersal modes are associated with the abundance of suitable disperers (e.g., birds, wind); and the resource-availability hypothesis, which suggests that zoochorous modes are more common in areas with sufficient temperature, precipitation, and soil fertility to support the production of costly fruits (Tabarelli et al., 2003; Correa et al., 2015). Questions remain as to whether the observed distribution of dispersal strategies is primarily driven by the availability of dispersers—such as wind intensity or frugivore abundance—or by environmental resource gradients that constrain the metabolic cost of fruit or seed production (Correa et al., 2023).

In temperate and boreal ecosystems, however, these relationships remain poorly quantified. Most work has focused on mutualistic dispersal interactions (e.g., frugivory and seed caching) rather than broader dispersal mode distributions (Chen et al., 2017). Moreover, few studies have considered how dispersal strategies co-vary with other plant traits, such as fruit type, seed mass, or plant height, or how these combinations shift across environmental gradients. Understanding these associations is essential for predicting plant responses to environmental change and informing conservation planning, especially in ecosystems where dispersal limitations may hinder recovery after disturbance (Clark et al., 1998; McConkey et al., 2012).

In this study, we examine the biogeographic and environmental patterns of plant dispersal modes across North American forests. Specifically, we ask: (1) Do dispersal mode distributions vary predictably with climate, topography, and disperser availability? (2) Are these patterns better explained by environmental constraints (resource-availability hypothesis) or by the presence of dispersal vectors (disperser-availability hypothesis)? (3) How do dispersal modes co-occur with other functional traits, and can these associations inform broader ecological strategies?

To answer these questions, we use a Predictive Trait Model (PTM) based on the Generalized Joint Attribute Modeling (GJAM) framework (Clark et al., 2017) to simultaneously model dispersal modes and multiple environmental and biotic predictors. By integrating trait data, NEON animal surveys, and spatial climate data, our study builds on tropical work such as Correa et al. (2023) to test these hypotheses in temperate and boreal systems. Our results offer new insights into the trait-environment relationships that shape plant dispersal strategies and highlight the importance of both environmental factors and disperser availability in structuring plant communities.

Methods

1 Model Structure

To examine the environmental and biotic drivers of dispersal mode distributions across temperate and boreal forests, we constructed a Predictive Trait Model (PTM) using the Generalized Joint Attribute Modeling (GJAM) framework (Clark et al., 2017). GJAM accommodates multivariate responses that include continuous, discrete, ordinal, zero-inflated, and censored data by mapping each response onto a continuous latent scale (Clark et al., 2017). This allows ecological interpretations to be made on the observation scale without relying on nonlinear link functions, enabling direct estimation of covariances among traits and predictors (Clark et al., 2017).

We implemented a multivariate response structure where the dispersal mode of tree species served as the response variable and the environmental (mean annual temperature, precipitation, wind speed, and topographic position index (TPI)) and biotic (disperser demand) covariates were predictors. The model formula was: Traits ~ PTM (precipitation + temperature + TPI + wind speed + dispersers demand).

2 Data Sources

Trait Data

Trait data for plant species were derived from Qiu et al. (2022), which includes traits linked to dispersal such as:

Trait	Unit	Description
Dispersal Modes	-	Mode type: anemochory (dispersed by wind), zoochory (dispersed by animal), hydrochory (dispersed by water), barochory (dispersed by gravity), both anemochory and zoochory
kCalPerGm	kcal/g	Seed Caloric energy content
Leaves	-	Leaf type (e.g., needleleaf evergreen, broadleaf deciduous)
Fruit	-	Fruit type: fleshy, capsule, nut, pod, winged
gmPerSeed	g	Seed mass
maxHt	m	Maximum height of the species

Table 1. *Description of plant traits used in the Predictive Trait Model (PTM). These traits are hypothesized to influence or co-vary with dispersal strategies across environmental gradients.*

The frequency of dispersal modes across the dataset was: anemochory (37.5%), zoochory (55%), hydrochory (2%), barochory (5%), and both (0.5%). Fruit categories were derived by collapsing related fruit types into ecologically meaningful groups (Table A1).

Plot Data

We used forest inventory plot data and lab plot data from the same dataset (Qiu et al., 2022) to determine species composition at each site. Each species' abundance was converted to a proportion of total plot composition and used in calculating community-weighted means for PTM modelling.

Environmental Predictors

Climate variables, including annual precipitation, temperature, and topographic position index (TPI), were extracted from plot data and averaged for 2022 across plot locations. Wind speed was averaged over a 10-year period (2008–2017) from the Global Wind Atlas at 250 m resolution and 50 m above ground (Global wind atlas, n.d., Figure A1).

Predictor	Unit	Source	Mean	Range
Precipitation	mm	Plot data average (2022)	80.00	12.69 – 150.1
Temperature	°C	Plot data average (2022)	12.27	-0.17 – 23.30
TPI	-	Plot data (2022)	-0.53	-60 - 53
Wind speed	m/s	Global Wind Atlas (2008–2017)	4.95	0.86 – 11.80
Disperser demand	g/ha	Calculated (see below)	36643.79	7154.708 - 207645.78

Table 2. *Summary of environmental and biotic predictors used in the Predictive Trait Model (PTM). Values represent the unit of measurement, data source, overall mean, and range across all forest plots included in the analysis. Climate variables reflect 2022 plot-level averages, wind speed is derived from a 10-year mean (2008–2017), and disperser demand is estimated based on frugivore and granivore density and diet.*

Disperser Demand Estimation

Disperser demand was estimated based on consumer density, body mass, and diet fraction using the formula: Demand (g/ha)=Density × Diet Fraction × Body Mass. We used NEON breeding landbird point counts survey (2025) and NEON small mammal box trapping (2025) to calculate birds' and small mammals' density. We calculated birds' and small mammals' demands for fruits and seeds separately and combined them for final modeling.

For bird density, we first estimated point-level demand and then aggregated point-level demand to the plot level by averaging across all points associated with each plot. Bird density was calculated with the formula: density = (n / p) / A, where: n = number of detections, p = detection probability, A = effective area (4.91 ha, based on a 250 m diameter point). Distance sampling was conducted using the Distance package in R (Miller et al., 2019). Truncation was set at 450 m (99% of observations; Buckland et al., 2001). Model selection for calculating detection probability followed recommendations from Buckland et al. (2001): Hazard-rate with simple

polynomial adjustments (AIC = 402201.86) was selected as the best model based on comparisons with uniform and half-normal functions. In cases with fewer than 20 detections per species, a general detection probability estimate from all bird species ($\hat{p} = 0.31$) was applied (Table A2). Small mammals density calculation follows similar procedure (Table A3).

Bird diet fractions were obtained from Dubovyk (2024) and birds body mass (in grams) is sourced from the lab trait dataset, updated with the Dunning dataset (WB3-update August 2023.xls., n.d.) and online searches for species not covered for bird. Small mammals' diet fraction and body mass were obtained from lab dataset.

Demand was calculated separately for fruit and seed dispersers (birds and mammals) and then summed to produce the final disperser_demand predictor. Results of bird and small mammals demand as dispersers are shown in Figure A2. Of 532 bird and 219 mammal points, 131 locations overlapped. For these, we selected the nearest forest plot within a 5 km radius, resulting in 97 valid points for the final model.

3 Analysis Workflow

We first visualized the geographic distribution of dispersal modes using all available plot data by generating distribution maps across the study region. To better understand the environmental conditions associated with different dispersal strategies, we constructed climate space plots, plotting environmental variables against the dispersal mode.

For statistical modeling, we ran the Predictive Trait Model (PTM) using the processed dataset that matched NEON animal survey sites with plot-level trait and climate data. Model outputs from the Generalized Joint Attribute Model (GJAM) were used to evaluate how plant traits and environmental conditions covary with dispersal modes.

To help interpretation of PTM results, we produced coefficient plots of posterior distributions for selected predictors across dispersal modes, highlighting effect size and uncertainty and a dendrogram to examine clustering relationships among plant traits used in the PTM. Trait distance matrices were computed using scaled values, and clustering was performed using hierarchical agglomerative methods. The dendrogram was constructed using the 'ggdendro' and 'dendextend' R packages (de Vries and Ripley, 2022; Galili, 2015), with visualization aided by ggplot2 (Wickham, 2016).

All analyses and visualizations were conducted in R (R Core Team, 2024). Spatial data were processed using base R functions and visualized using ggplot2. All code was documented for reproducibility.

Results

Geographic Patterns of Dispersal Modes

The geographic distribution of dispersal modes, visualized as community-weighted means (CWMs) weighted by mean fecundity (g/ha), reveals distinct spatial patterns across North America (Figure 1). Zoochory (animal dispersal) dominates in the southeastern United States

and other low-latitude regions, especially in eastern deciduous forests and southern mixed woodlands. Its prevalence decreases toward higher latitudes and more arid or open landscapes in the west. In contrast, anemochory (wind dispersal) shows an inverse pattern, with greater representation in northern latitudes and western interior regions such as the boreal forests and Great Plains.
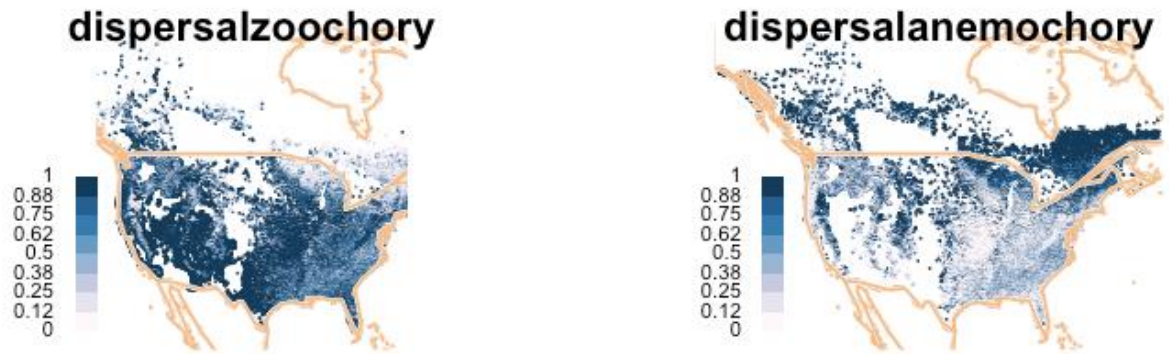

Figure 1. *Geographic distribution of zoochory and anemochory across North America. Values represent the proportion of each dispersal mode within communities, weighted by mean fecundity (g/ha). Darker colors indicate higher community-weighted representation of the dispersal mode. Maps highlight the latitudinal gradient, with zoochory concentrated in lower latitudes and anemochory more common in northern and interior regions.*

Climatic Space of Dispersal Modes

The climate space distribution of zoochory and anemochory, plotted using mean annual temperature (°C) and mean monthly water deficit (mm), reveals distinct ecological niches for each dispersal strategy (Figure 2). Zoochorous species tend to dominate in warmer and wetter regions, clustering in areas with higher mean annual temperatures and lower water deficits, consistent with environments that support frugivorous animal communities. In contrast, anemochorous species are more prominent in cooler and drier climates, particularly in regions with elevated water deficits and lower mean temperatures.
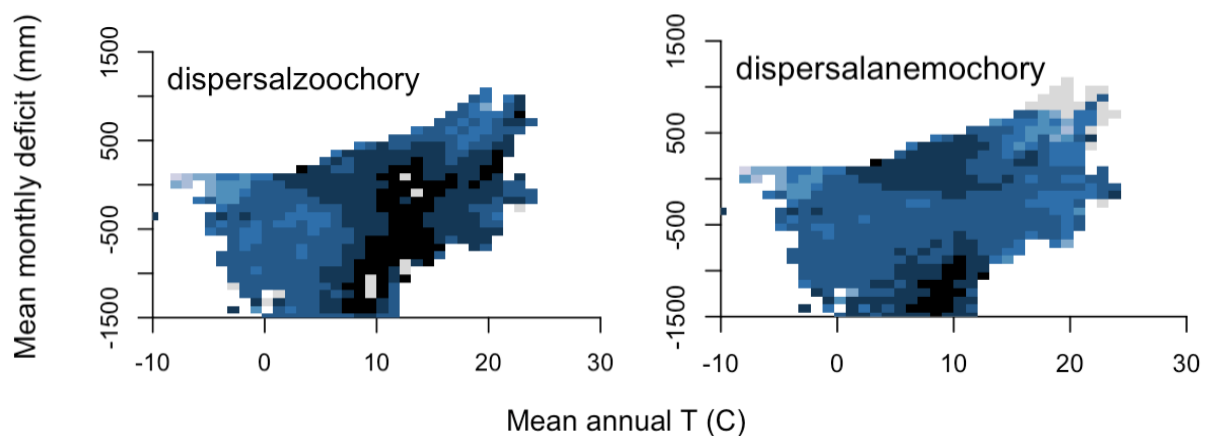

Figure 2. *Climatic space for zoochory and anemochory across North America. Each pixel represents a cell in mean annual temperature (°C) and mean monthly water deficit (mm) space, with shading indicating mean fecundity (g/ha) for communities dominated by each dispersal mode. Darker pixels correspond to higher fecundity values. Zoochory peaks in warm, low-deficit climates, while anemochory is more prevalent in cooler, water-limited environments.*

Model Estimates for Environmental Drivers of Dispersal Modes

Posterior estimates from the Predictive Trait Model (PTM) identified distinct environmental correlates for zoochory and anemochory (Figure 3). For zoochory (top panel), the most influential predictor was wind speed, with a mean estimate of –1.27 (95% CI: –3.63 to 1.42), indicating a generally negative association between zoochory and high wind environments. Temperature also showed a negative effect (–0.472; CI: –1.36 to 0.29), while precipitation had a small negative estimate (–0.088; CI: –0.184 to 0.017), suggesting that zoochorous species may be less prevalent in drier or cooler areas. The effects of TPI (0.211; CI: –0.017 to 0.416) and disperser demand (6.88×10^{-6}; CI: $–1.41 \times 10^{-4}$ to 2.10×10^{-4}) were weak and negligible.

For anemochory (bottom panel), wind speed had a slightly positive effect (0.0098; CI: –1.63 to 1.70), but the wide credible interval suggests substantial uncertainty. Temperature had the strongest estimate among all predictors (0.462; CI: –0.377 to 1.22), indicating a possible positive association with anemochorous strategies in warmer regions. Precipitation (–0.0105), TPI (0.142), and disperser demand (7.06×10^{-5}) showed minimal effects with confidence intervals that include zero, suggesting limited evidence for strong directional influences from these variables. Together, these results indicate directional association with ecological expectations, but the high degree of posterior uncertainty limits definitive interpretation.
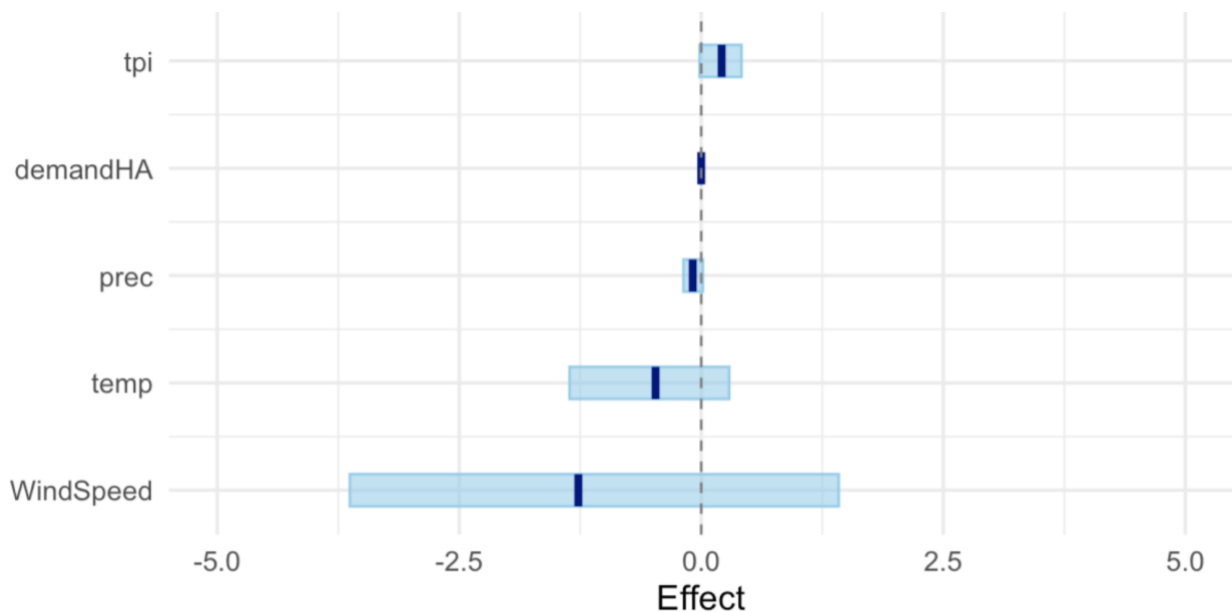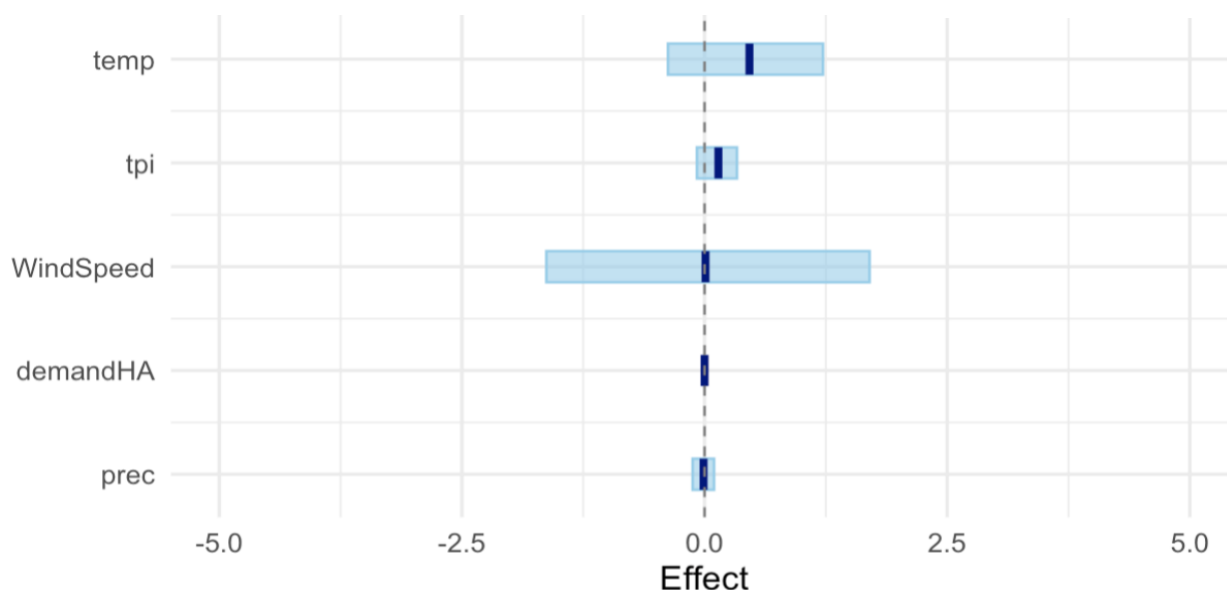

Zoochory

Figure 3. *Posterior distributions of predictor coefficients from the Predictive Trait Model (PTM) for zoochory (top) and anemochory (bottom). Bars represent 95% credible intervals. Although wind speed and temperature show the strongest effects in both models, none of the predictors are statistically significant (credible intervals all include zero). Detailed coefficient values and uncertainty bounds are provided in Table A4.*

Trait Response Similarities Based on Predictor Effects

The dendrogram generated from model output visualizes the similarity in how different traits respond to the set of environmental predictors in the PTM, rather than direct correlations between traits themselves (Figure 4; Clark, 2024). Dispersal modes appear across different branches, indicating contrasting environmental response profiles. For example, anumochory clusters closely with traits such as needle-leaved evergreen foliage and winged fruit, consistent with traits that are typically adapted to open, seasonal, or high-wind environments. In contrast, zoochory is grouped nearer to fleshy fruit types and broad-leaved deciduous species, reflecting trait syndromes commonly associated with animal-mediated dispersal in mesic forest environments. Interestingly, barochory clusters with needle-leaved deciduous species, which indicate adaptation to harsh, nutrient-poor, or drought-prone habitats, where traits such as needle-leaved deciduous and minimal dispersal investment (barochory) are beneficial.

This dendrogram emphasizes how different dispersal strategies co-occur with specific ecological traits under similar environmental gradients, potentially pointing to functional trait combinations that enhance performance under given conditions. As emphasized by Clark (2023), the clustering reflects trait responses to predictors rather than intrinsic trait similarities, providing a valuable framework for interpreting the ecological assembly of trait syndromes in plant communities.
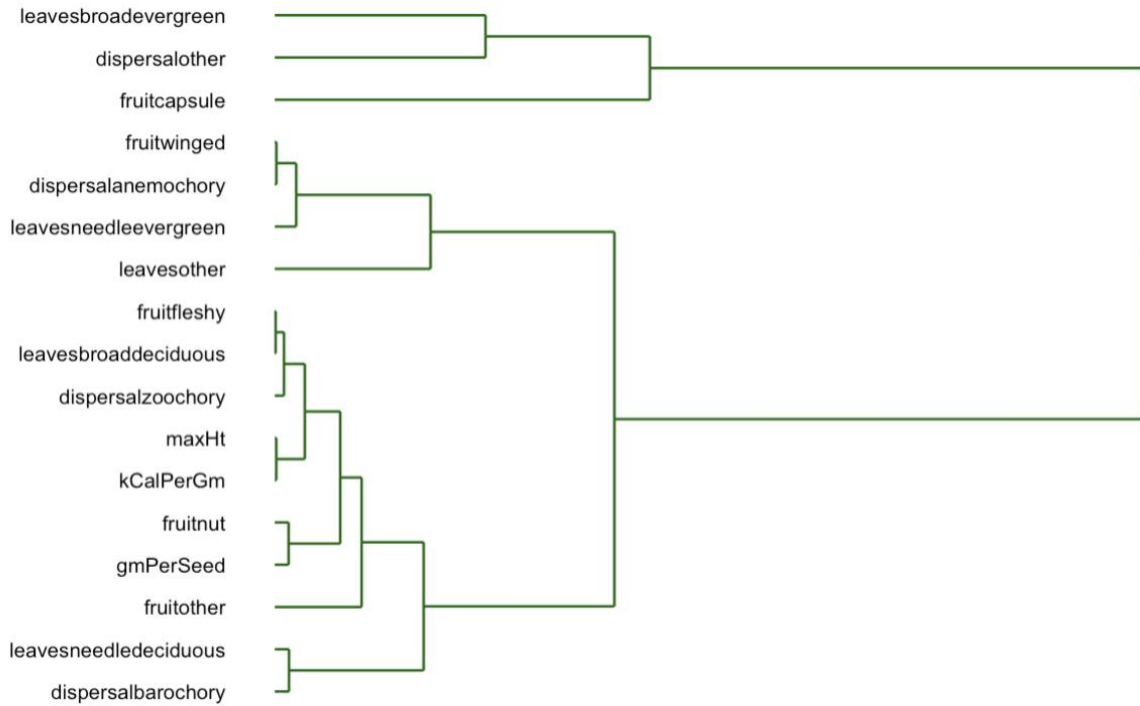
Figure 4. *Hierarchical clustering of traits based on similarity in response to environmental predictors in the PTM. The dendrogram reflects shared patterns in model coefficients rather than direct trait correlations. Dispersal modes form distinct clusters: anemochory with needle leaves and winged fruits, zoochory with fleshy fruits and broad leaves.*

Wind Speed Effects Relative to Seed and Height

To further explore trait-based variation in wind-mediated dispersal, we examined species-specific estimates of wind speed effects from the PTM in relation to seed mass and maximum plant height for anemochorous species (Figure 5). The first plot displays wind speed effect estimates against maximum height, while the second relates them to seed mass (g/seed). Despite theoretical expectations that taller plants or lighter seeds should benefit more from wind dispersal due to prolonged airborne time and reduced terminal velocity (Greene & Johnson, 1989; Tackenberg, 2003), no clear relationship emerges in either case.

Across a wide range of maximum heights (10–60 m), wind speed effect estimates fluctuate without a consistent pattern. Similarly, wind speed estimates do not align clearly with seed mass. Most species cluster around very small seed sizes (<0.1 g), but their wind response estimates vary from slightly negative to moderately positive. One outlier, Pinus sabiniana, has a notably larger seed mass (0.55 g) and a strongly negative wind effect estimate, but it alone does not define a broader trend.

However, when evaluating the full species-level results (Table A5), certain taxonomic patterns and individual species stand out. Most acer species consistently exhibit positive wind speed estimates, including Acer pensylvanicum (0.0589), Acer rubrum (0.0238), Acer saccharum (0.0407), and Acer spicatum (0.0569), with two (Acer pensylvanicum and Acer spicatum) showing statistically significant positive effects. These results align with their known morphological adapted samaras that facilitate wind dispersal. In contrast, Platanus

11

occidentalis showed a significant negative effect of wind speed (–0.0443; 95% CI: –0.0859 to –0.00276), suggesting lower dispersal success in windy environments despite being classified as anemochorous. Similarly, several conifer species including Pinus taeda and Pinus sabiniana had negative wind speed effects, though these were not statistically significant. Conversely, several species showed strong positive but non-significant wind responses, including Thuja plicata (0.046), Picea mariana (0.0446), and Tsuga heterophylla (0.0428), possibly reflecting adaptation to high-elevation or high-wind habitats where such traits offer a selective advantage.

Relationship between Wind Speed Estimate and Max Height (Anemochory Species)
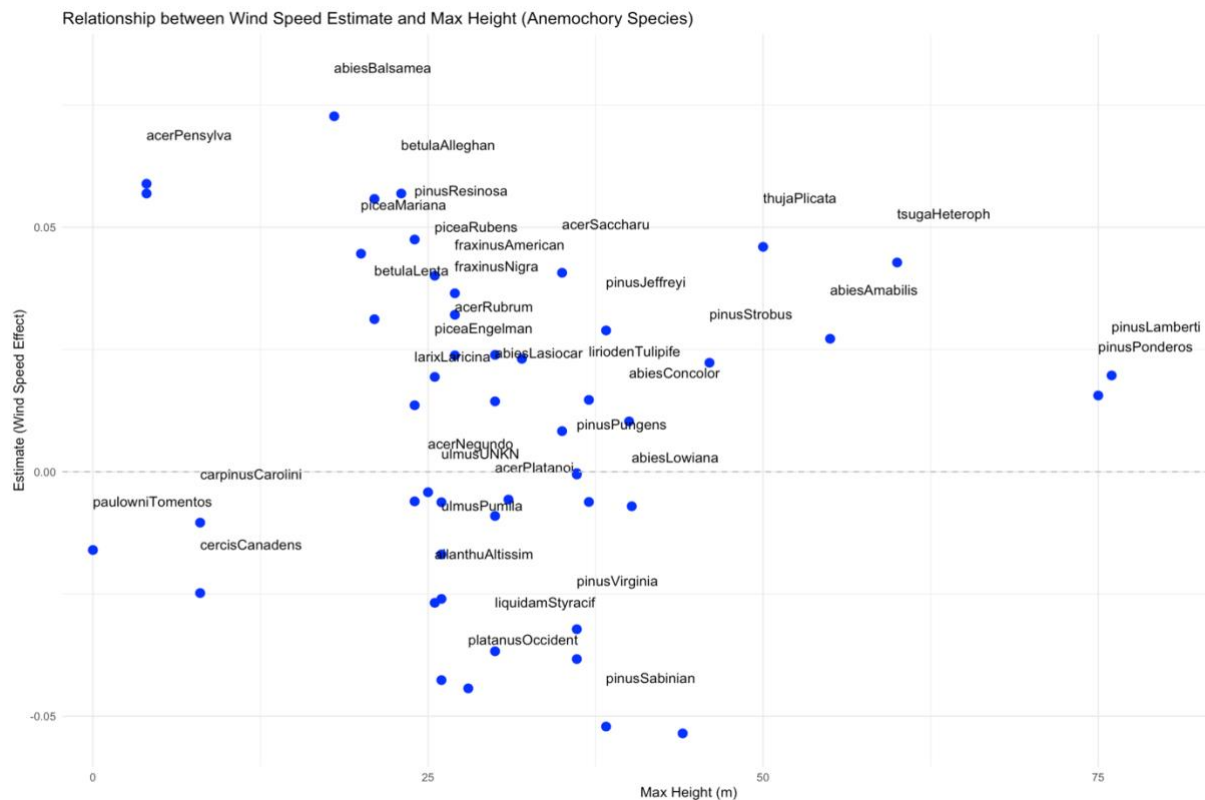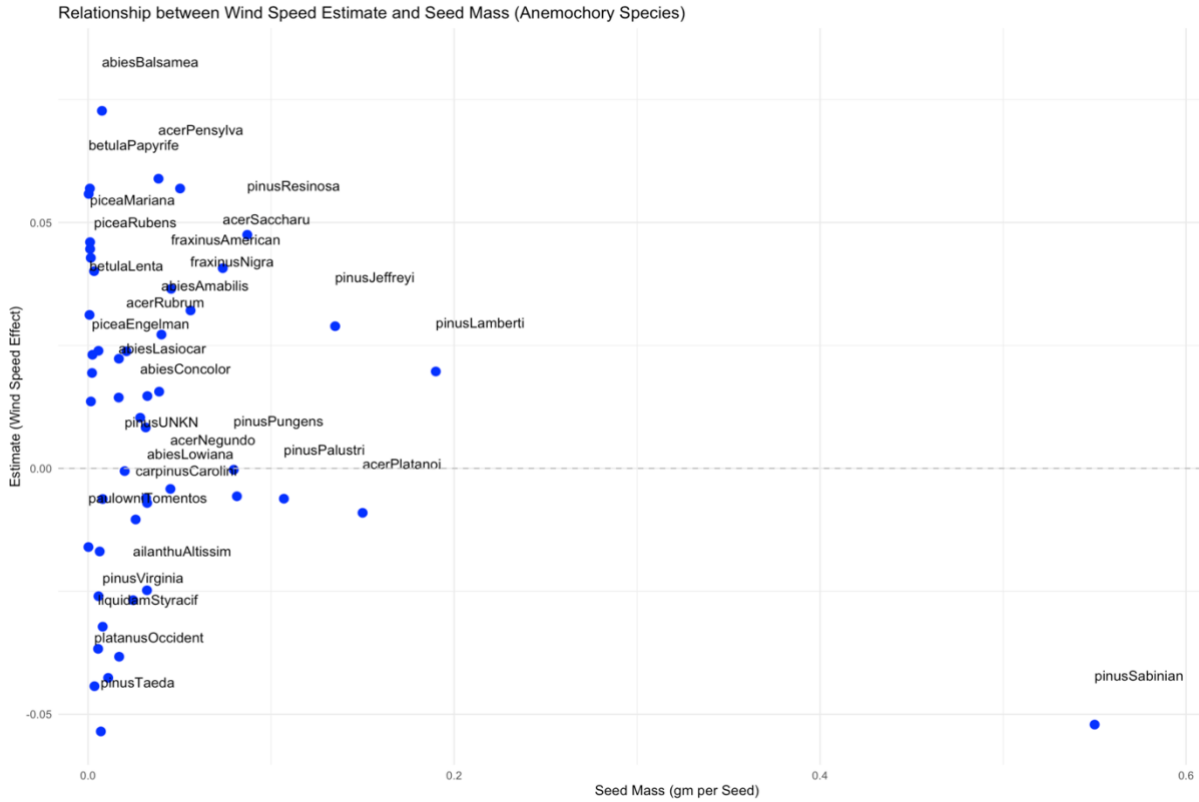
Figure 5. Species-level wind speed effect estimates for anemochorous plants plotted against seed mass (bottom) and maximum height (top). While no strong linear relationships are observed, several taxonomic and functional groups (e.g., Acer species, conifers) show consistent patterns in wind response. Significant effects are noted for both positive and negative associations (see Table A5).

Discussion

Our observation map reveals strong geographic and climatic partitioning of plant dispersal modes across North America. Zoochory dominates in warmer, low-latitude regions while anemochory increases with latitude and in more open, seasonally dry ecosystems. These findings support long-standing biogeographic patterns observed globally, where animal dispersal is prevalent in species-rich tropical and subtropical ecosystems (Correa et al., 2023; Moles et al., 2007; Chen et al., 2017), and wind dispersal becomes increasingly dominant at higher latitudes and elevations, particularly in open or seasonal biomes (Correa et al., 2023).

The observed climate space separation further underscores the ecological divergence of these strategies: zoochory clusters in warm, low-deficit environments conducive to frugivory, while anemochory occupies cooler, water-limited conditions. This aligns with theoretical expectations that frugivorous animals are more abundant and active in mesic environments (Russo and Chapman, 2011), while abiotic dispersal mechanisms become more dominant under limiting environmental constraints (Nathan & Muller-Landau, 2000).

Despite these clear biogeographic trends, our PTM results show considerable uncertainty in the statistical relationships between environmental predictors and dispersal modes. While zoochory showed a negative association with wind speed, temperature, and precipitation, and

anemochory showed weakly positive associations with wind and temperature, none of these predictors had statistically significant effects. These results diverge slightly from prior findings in tropical systems where wind strongly correlates with dispersal mode (Correa et al., 2023). One explanation for this may lie in the greater climatic and ecological heterogeneity of temperate systems, where dispersal modes are influenced by multiple interacting variables—including disturbance history, forest structure, and disperser presence—making coarse-scale climatic predictors insufficient. Additionally, zoochory's weak association with disperser demand in our model suggests that simple biomass- or density-based metrics may not adequately capture the behavioral or functional capacity of animal dispersers (Sheard et al., 2020). For instance, a bird's hand-wing index may need to be involved in our demand equation to consider different dispersal ability for different species (Sheard et al., 2020).

The trait dendrogram revealed coherent functional groupings aligned with dispersal syndromes. Anemochory clustered with needle-leaved evergreen foliage and winged fruits—traits typical of wind-dispersed species in open or seasonal environments (Augspurger, 1986). In contrast, zoochory aligned with fleshy fruits and broad leaves, consistent with adaptation to frugivory. Barochory's association with needle-leaved deciduous species may suggests a distinct ecological strategy: minimal dispersal investment, likely advantageous in resource-poor, stable environments such as alpine or boreal systems (Moles & Westoby, 2004). These trait-based groupings support the idea that environmental filters promote the co-occurrence of functional traits, reinforcing that dispersal mode is rarely independent but part of broader ecological strategies involving life history, resource use, and reproductive investment (Westoby et al., 2002; Cornwell & Ackerly, 2009; Götzenberger et al., 2012).

While wind dispersal is commonly modeled using proxies such as seed mass or plant height, our analysis of anemochorous species reveals that these traits alone poorly predict wind response. Across a wide range of plant sizes and seed masses, wind speed effects remain highly variable—echoing previous research showing that effective wind dispersal is governed by a complex interplay of structural and aerodynamic traits, including seed terminal velocity, surface morphology, drag, release height, and wind regime characteristics (Nathan et al., 2002; Tackenberg, 2003).

A surprising result was the weak or even slightly positive association between wind speed and anemochory, despite theoretical concerns that strong winds could hinder rather than help gliding seeds. Indeed, while moderate winds facilitate horizontal seed displacement, excessively strong or turbulent winds may induce erratic seed trajectories or cause premature descent (Nathan et al., 2002). For gliding or autorotating seeds like samaras, optimal dispersal may occur under intermediate conditions where vertical lift and lateral transport are balanced (Augspurger, 1986; Katul et al., 2005). The coarse temporal and spatial averaging of wind speed in our dataset (10-year mean at 50 m height) may also obscure finer-scale effects. For example, gustiness or canopy-level turbulence during the seed release window may be more ecologically relevant than long-term mean wind speeds (Soons et al., 2004; Thomson et al., 2011).

Conclusion

Seed dispersal is a fundamental ecological process that influences plant community structure and enables species to respond to environmental change. By examining the geographic and

environmental structuring of dispersal modes across North America, this study offers new insights into the drivers of variation in plant dispersal strategies beyond tropical ecosystems, which have been the primary focus of most previous research.

Our findings provide partial support for both the resource-availability and disperser-availability hypotheses. Dispersal mode distributions showed clear geographic and climatic structuring, with zoochory concentrated in warmer, wetter environments and anemochory more common in cooler, drier, and higher-wind regions. These patterns suggest that both environmental constraints and disperser availability shape broad-scale distributions. However, the relatively weak statistical associations in our model highlight the complexity of these interactions and the potential for unmeasured factors—such as forest structure, disturbance regimes, and fine-scale disperser behavior—to influence outcomes. Moreover, the co-occurrence of dispersal modes with suites of functional traits (e.g., zoochory with fleshy fruits and broad leaves; anemochory with winged fruits and needle-leaved evergreen foliage) reinforces the idea that dispersal strategies are embedded within broader ecological syndromes. Together, these insights underscore the importance of considering multiple axes of trait and environmental variation when predicting species' dispersal capacities and responses to environmental change.

Methodologically, this study introduces a novel approach for estimating animal disperser availability by integrating diet, body size, and density data into a predictive trait model. This represents a step toward more mechanistic models of plant-disperser interactions. However, at the same time, it underscores current data gaps and several important limitations. First, we do not distinguish forest types or ecoregions, which could introduce bias as dispersal strategies are often constrained by local biome conditions (Correa et al., 2023). Second, the analysis does not account for species with multiple dispersal vectors (e.g., those exhibiting both zoochory and barochory) or the occurrence of long-distance dispersal events, both of which play crucial roles in colonization processes and range expansion (Nathan et al., 2008; Jordano et al., 2007). Our disperser demand variable may also oversimplify complex plant-animal interactions. For example, differences in flight morphology (e.g., wing shape in birds) can influence dispersal potential (Sheard et al., 2020). Furthermore, the bird density estimates derived from distance sampling carry their own assumptions and limitations. A uniform truncation distance was applied across all species, potentially masking differences in detectability among species with distinct vocalization or behavior. For species with fewer than 20 detections, we applied an average detection probability ($\hat{p} = 0.31$), which may not accurately reflect species-specific detectability. As with all distance sampling approaches, the method assumes perfect detection at 0 m and accurate distance measurements from observers—assumptions that may not hold consistently in the field. Additionally, our animal disperser dataset was constrained by the spatial overlap between NEON animal observations and plot-level trait data, limiting sample size and potentially excluding relevant disperser species. Expanding the spatial and taxonomic coverage of frugivore and granivore data would improve estimates of disperser availability and ecological interactions. Finally, wind speed is averaged across a decade and does not account for interannual variation or conditions during seed release periods, which are often critical windows for dispersal success. Moving forward, further studies are needed to improve spatial and temporal resolution of disperser and wind data, incorporating multiple dispersal modes, and expanding trait coverage.

References

Almeida-Neto, M., Campassi, F., Galetti, M., Jordano, P., & Oliveira-Filho, A. (2008). Vertebrate dispersal syndromes along the Atlantic forest: broad-scale patterns and macroecological correlates. Global Ecology and Biogeography, 17(4), 503-513.

Augspurger, C. K. (1986). Morphology and dispersal potential of wind-dispersed diaspores of neotropical trees. *American Journal of Botany, 73*(3), 353–363.

Buckland, S. T., Anderson, D. R., Burnham, K. P., & Laake, J. L. (2001). Introduction to Distance Sampling. Oxford University Press.

Russo, S. E., & Chapman, C. A. (2011). Primate seed dispersal: Linking behavioral ecology with forest community structure. Primates in perspective, 2, 523-534.

Chen, S. C., Cornwell, W. K., Zhang, H. X., & Moles, A. T. (2017). Plants show more flesh in the tropics: Variation in fruit type along latitudinal and climatic gradients. Ecography, 40(4), 531–538.

Clark, J. S. (2024). *16. Traits*. RPubs. https://rpubs.com/jimclark/1171526

Clark, J. S., Fastie, C., Hurtt, G., Jackson, S. T., Johnson, C., King, G. A., ... & Wyckoff, P. (1998). Reid's paradox of rapid plant migration: dispersal theory and interpretation of paleoecological records. BioScience, 48(1), 13-24.

Clark, J. S., Nemergut, D., Seyednasrollah, B., Turner, P., & Zhang, S. (2017). Generalized joint attribute modeling for biodiversity analysis: Median-zero, multivariate, multifarious data. Ecological Monographs, 87(1), 34–56.

Connell, J. H. (1971). On the role of natural enemies in preventing competitive exclusion in some marine animals and in rain forest trees. *Dynamics of Populations*, 298–312.

Corlett, R. T., & Westcott, D. A. (2013). Will plant movements keep up with climate change? *Trends in Ecology & Evolution, 28*(8), 482–488.

Cornwell, W. K., & Ackerly, D. D. (2009). *Community assembly and shifts in plant trait distributions across an environmental gradient in coastal California.* Ecological Monographs, 79(1), 109–126.

Correa, D. F., Rey-Benayas, J. M., & Meli, P. (2023). Geographic patterns of tree dispersal modes in Amazonia and their ecological correlates. *Global Ecology and Biogeography, 32*(1), 49–69.

de Vries A, Ripley B. 2022. ggdendro: Create Dendrograms and Tree Diagrams Using ggplot2. R package version 0.1.23. https://CRAN.R-project.org/package=ggdendro,

Dubovyk, O. (2024). Functional traits database for North American birds [Data set]. Zenodo. https://doi.org/10.5281/zenodo.13351162

Galili T. 2015. dendextend: an R package for visualizing, adjusting and comparing trees of hierarchical clustering. *Bioinformatics*. 31(22):3718–3720. https://doi.org/10.1093/bioinformatics/btv428

Global Wind Atlas. (n.d.). https://globalwindatlas.info/en/area/United%20States

Götzenberger, L., et al. (2012). *Ecological assembly rules in plant communities—approaches, patterns and prospects.* Biological Reviews, 87(1), 111–127.

Greene, D. F., & Johnson, E. A. (1989). A model of wind dispersal of winged or plumed seeds. *Ecology, 70*(2), 339–347

Howe, H. F., & Smallwood, J. (1982). Ecology of seed dispersal. *Annual Review of Ecology and Systematics, 13*, 201–228.

Janzen, D. H. (1970). Herbivores and the number of tree species in tropical forests. *The American Naturalist, 104*(940), 501–528.

Jordano, P., García, C., Godoy, J. A., & García-Castaño, J. L. (2007). *Differential contribution of frugivores to complex seed dispersal patterns.* Proceedings of the National Academy of Sciences, 104(9), 3278–3282.

Katul, G. G., Porporato, A., Nathan, R., Siqueira, M., Soons, M. B., Poggi, D., ... & Horn, H. S. (2005). Mechanistic analytical models for long-distance seed dispersal by wind. *The American Naturalist, 166*(3), 368–381.

McConkey, K. R., et al. (2012). Seed dispersal in changing landscapes. *Biological Conservation, 146*(1), 1–13.

Miller, D. L., Rexstad, E., Thomas, L., Marshall, L., & Laake, J. L. (2019). Distance sampling in R. Journal of Statistical Software, 89(1), 1–28.

Moles, A. T., & Westoby, M. (2004). Seedling survival and seed size: A synthesis of the literature. *Journal of Ecology, 92*(3), 372–383.

Moles, A. T., Ackerly, D. D., Tweddle, J. C., Dickie, J. B., Smith, R., Leishman, M. R., Mayfield, M. M., Pitman, A., Wood, J. T., & Westoby, M. (2007). Global patterns in seed size. Global Ecology and Biogeography, 16(1), 109–116.

Nathan, R., & Muller-Landau, H. C. (2000). Spatial patterns of seed dispersal, their determinants and consequences for recruitment. *Trends in Ecology & Evolution, 15*(7), 278–285.

Nathan, R., Katul, G. G., Horn, H. S., Thomas, S. M., Oren, R., Avissar, R., ... & Levin, S. A. (2002). *Mechanisms of long-distance dispersal of seeds by wind.* Nature, 418, 409–413. https://doi.org/10.1038/nature00844

Nathan, R., Schurr, F. M., Spiegel, O., Steinitz, O., Trakhtenbrot, A., & Tsoar, A. (2008). Mechanisms of long-distance seed dispersal. *Trends in Ecology & Evolution, 23*(11), 638–647. https://doi.org/10.1016/j.tree.2008.08.003

NEON (National Ecological Observatory Network). Breeding landbird point counts (DP1.10003.001), RELEASE-2024. https://doi.org/10.48443/4a0h-fy23. Dataset accessed from https://data.neonscience.org/data-products/DP1.10003.001/RELEASE-2024 on January 8, 2025.

NEON (National Ecological Observatory Network). Small mammal box trapping (DP1.10072.001), RELEASE-2025. https://doi.org/10.48443/yrh2-6058. Dataset accessed from https://data.neonscience.org/data-products/DP1.10072.001/RELEASE-2025 on February 18, 2025.

OpenAI. (2024). ChatGPT (Mar 2024 version) [Large language model]. https://chat.openai.com/

Qiu, T., Andrus, R., Aravena, M. C., Ascoli, D., Bergeron, Y., Berretti, R., ... & Clark, J. S. (2022). Limits to reproduction and seed size-number trade-offs that shape forest dominance and future recovery. Nature Communications, 13(1), 2381.

R Core Team. 2024. *R: A Language and Environment for Statistical Computing*. R Foundation for Statistical Computing, Vienna, Austria.

Sheard, C., Neate-Clegg, M. H., Alioravainen, N., Jones, S. E., Vincent, C., MacGregor, H. E., ... & Tobias, J. A. (2020). Ecological drivers of global gradients in avian dispersal inferred from wing morphology. *Nature Communications, 11*, 2463.

Tabarelli, M., & Peres, C. A. (2002). Abiotic and vertebrate seed dispersal in the Brazilian Atlantic forest: Implications for forest regeneration. *Biological Conservation, 106*(2), 165–176. https://doi.org/10.1016/S0006-3207(01)00243-9

Tackenberg, O. (2003). Modeling long-distance dispersal of plant diaspores by wind. *Ecological Monographs, 73*(2), 173–189.

WB3-update August 2023.xls. (n.d.). Google Docs. https://docs.google.com/spreadsheets/d/1GjoJk2LhVy-ilJJPwR8Ff6UNta_TiMsp/edit?gid=917927225#gid=917927225

Westoby, M., Falster, D. S., Moles, A. T., Vesk, P. A., & Wright, I. J. (2002). Plant ecological strategies: Some leading dimensions of variation between species. *Annual Review of Ecology and Systematics, 33*, 125–159.

Wickham H. 2016. *ggplot2: Elegant Graphics for Data Analysis*. Springer-Verlag New York.

Willson, M. F., Irvine, A. K., & Walsh, N. G. (1989). Vertebrate dispersal syndromes in some Australian and New Zealand plant communities, with geographical comparisons. *Biotropica, 22*(2), 133–147. https://doi.org/10.2307/2388412

Appendix

Table A1. Reclassification of original fruit types into broader ecological categories used in the analysis. Groupings reflect morphological traits linked to dispersal mechanisms.

Reclassified Category	Original Fruit Types Merged
Fleshy	syncarpium, pome, berry, berry-cone, drupe, fleshy fruit
Winged	achenosum, samara, winged drupe, winged nut
Nut	nutlet
Capsule	capsule
Pod	pod

Figure A1. Wind speed distribution used in analysis.

Left: Map of mean annual wind speed (2008–2017) at 50 m above ground across North America, obtained from the Global Wind Atlas. Color gradient indicates wind speed in m/s, with red/orange indicating higher wind regions (e.g., coastal and mountainous areas).
Right: Mean wind speed as a function of the percentile of windiest areas. The plot shows that the windiest 10% of locations exceed 8.5 m/s, with a steady decline across the remaining landscape. These data were used as predictors in the PTM to evaluate environmental influences on dispersal mode.
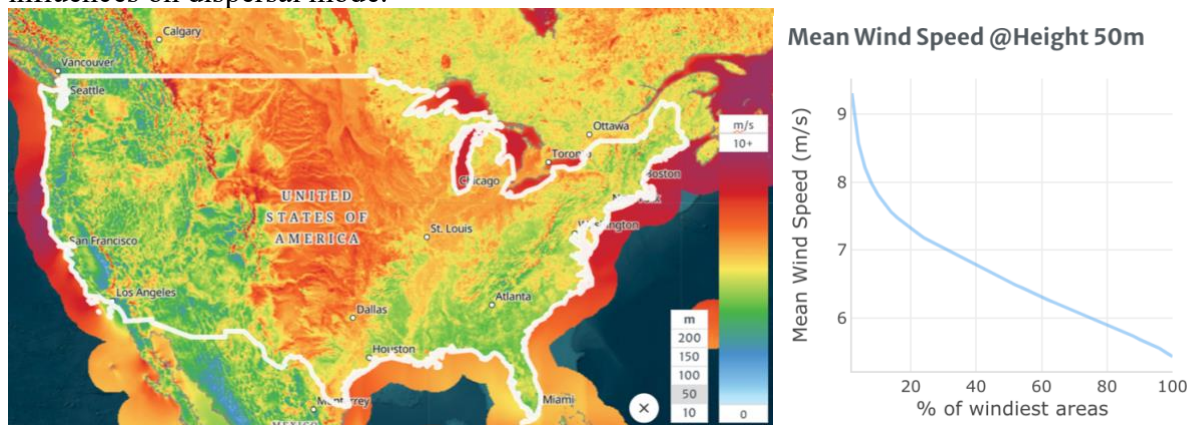
Table A2. Bird species detection probabilities and estimated densities used to calculate disperser demand. Detection probabilities ($\hat{p}$) and standard errors (SE) are derived from distance sampling. Only a subset of species is shown here due to space constraints. Plot-level estimates of frugivore and granivore demand (g/ha) below are based on species-level diet fractions, body mass, and detection-adjusted density. Full table includes >500 rows; only the first several rows are displayed here as an example.

scientificName	p_hat	se_hat	n_detections
Cyanocitta cristata	0.42174596	0.0149244	348
Vireo olivaceus	0.18507039	0.00329695	1422
Troglodytes hiemalis	0.1862124	0.01526735	59
Catharus guttatus	0.34727464	0.01486059	238
Seiurus aurocapilla	0.18504635	0.00370677	819
Sitta canadensis	0.25389794	0.02225704	306
Setophaga virens	0.1819007	0.0058505	278

Vireo solitarius	0.13597013	0.01103439	106
Setophaga fusca	0.09982215	0.00644197	85
Certhia americana	0.13779815	0.00885611	102
Poecile atricapillus	0.22994129	0.01705118	133
Sphyrapicus varius	0.26534681	0.01418452	110
Catharus ustulatus	0.28924054	0.00755021	359
Zenaida macroura	0.37819043	0.00940783	1325
Coccyzus erythropthalmus	0.31072678	NA	5
Catharus fuscescens	0.20775635	0.00955675	199
Piranga olivacea	0.26575947	0.00949533	215
Setophaga americana	0.1434305	0.00518275	323
Setophaga caerulescens	0.13694121	0.00955135	91
Contopus virens	0.30045822	0.01147204	353
Haemorhous purpureus	0.31072678	NA	11
Picoides villosus	0.26149817	0.01550656	114
Pheucticus ludovicianus	0.22655286	0.01903214	44
Dryocopus pileatus	0.51469207	0.02424304	166
Corvus corax	0.80902161	0.03651302	262
Aves sp.	0.17466929	0.01616377	156
Buteo platypterus	0.31072678	NA	12
Setophaga coronata	0.25345858	0.00637558	373
Mniotilta varia	0.16276003	0.00789348	192
Setophaga pensylvanica	0.15174485	0.00832994	147
Sitta carolinensis	0.2676877	0.01004084	274
Picoides pubescens	0.20036434	0.01528383	95
Setophaga pinus	0.17685073	0.00577701	299
Regulus satrapa	0.14355261	0.00786821	127
Picidae sp.	0.49089733	0.02336476	153
Junco hyemalis	0.23932956	0.00572846	491
Oreothlypis ruficapilla	0.19251046	0.01136032	149
Setophaga ruticilla	0.1415674	0.007077	149
Myiarchus crinitus	0.33963558	0.01670197	404
Hylocichla mustelina	0.35952557	0.01607976	177
Geothlypis trichas	0.28682311	0.01304005	242
Pipilo erythrophthalmus	0.22621382	0.00616069	448
Empidonax minimus	0.15028924	0.00970321	124
Baeolophus bicolor	0.30817318	0.0068575	835
Meleagris gallopavo	0.76420988	0.12975316	44
Turdus migratorius	0.39549696	0.01482909	339
Bonasa umbellus	0.31072678	NA	9
Melanerpes carolinus	0.35213249	0.01160395	499
Agelaius phoeniceus	0.45896291	0.02468607	401

| Quiscalus quiscula | 0.31512706 | 0.03305483 | 79 |
| Gavia sp. | 0.31072678 | NA | 14 |

Plot-level estimates

plotID	Frugivore demand (g/HA)	Granivore demand (g/HA)	Mean density per HA	Mean density
ABBY_001	8220.20704	3044.13952	1.15970607	0.05562181
ABBY_002	5398.1373	24668.2178	1.10618214	0.07524953
ABBY_003	5609.6185	26685.3832	1.10570091	0.03890937
ABBY_004	7034.71912	21756.972	0.88543209	0.04629197
ABBY_006	3323.00048	2954.05427	1.14156957	0.05215134
ABBY_007	28178.6579	19423.4543	1.36193522	0.05926907
ABBY_008	4887.2868	9752.92473	1.33079722	0.04596873
ABBY_009	6267.03507	19961.0238	1.07646946	0.07470086
ABBY_010	6292.97033	23401.9875	1.2422443	0.03221712
ABBY_011	8731.11162	29706.1272	1.48852667	0.03731556
ABBY_013	6510.98285	45079.2198	1.34355165	0.03898758
ABBY_014	5595.22071	11922.7709	0.91130644	0.05698815
ABBY_016	3356.29356	2645.62388	1.28842471	0.03969223
ABBY_017	9379.50245	1886.91485	1.53701701	0.03766809
ABBY_018	9318.86448	32747.988	1.30301463	0.03869887
ABBY_019	3958.5977	5178.51233	0.69862758	0.04584429
ABBY_020	5304.70846	21333.1593	0.70386351	0.02194867
ABBY_023	2914.45947	64456.1493	1.74767632	0.05649894
ABBY_077	4908.03652	23941.1359	1.04359609	0.03582105
BARR_021	0	136.122952	0.64163062	0.00812956
BARR_031	0	204.184428	0.47731425	0.00233368
BARR_034	0	51.0461069	0.37124441	0.00106067
BARR_035	0	90.7486346	0.49499255	0.00117078
BARR_038	0	294.933062	0.68945391	0.00277453
BARR_039	0	272.245904	0.55686662	0.00282007
BART_003	2538.30712	1681.21404	1.21142068	0.00801082
BART_004	2414.41879	1683.84865	1.36157271	0.00874181
BART_009	2439.72023	2031.65495	1.30764867	0.00877456
BART_012	1714.14277	1334.38012	1.31742103	0.00801832
BART_015	2532.05745	1275.20035	1.39706149	0.00969998
BART_016	3117.59093	2041.81485	1.36363353	0.00935031
BART_018	3214.22528	3025.00255	1.18541502	0.00926791
BART_025	2468.54864	2482.25769	1.00959891	0.01051532
BART_082	2561.02484	3022.51041	1.22097124	0.01074444
BLAN_001	6307.8703	27509.5844	1.54484342	0.01436936

BLAN_003	13363.6069	32473.7926	0.99306438	0.01396014
BLAN_004	43031.1635	58812.4021	1.08002207	0.01557985
BLAN_005	9142.54466	4840.26613	1.32041974	0.0153124

Table A3. Plot-level estimates of animal disperser demand across NEON forest plots. Values represent estimated frugivore and granivore demand in grams per hectare (g/ha) for each plot, based on NEON small mammal survey data. Decimal latitude and longitude indicate the geographic location of each plot centroid. Only display subset of the table due to space limitation.

plotID	Frugivore demand (g/HA)	Granivore demand (g/HA)	decimalLatitude	decimalLongitude
ABBY_002	9572.10714	14839.1786	45.740362	-122.30974
ABBY_004	6302.78571	13504.2857	45.76854	-122.30036
ABBY_007	2871.5	2871.5	45.768772	-122.36299
ABBY_010	2659.27778	3341.33333	45.777213	-122.37368
ABBY_014	661.5	661.5	45.749698	-122.31731
ABBY_023	4680.5	4680.5	45.746374	-122.3814
BART_001	5810	8346	44.046877	-71.305115
BART_007	4042	4696	44.051112	-71.298377
BART_012	17116.2857	21318.8571	44.047478	-71.315451
BART_015	8700.33333	13587.3333	44.042898	-71.275059
BART_062	13003.6	14644	44.05735	-71.308646
BART_084	8206	11999	44.048501	-71.297965
BLAN_001	5827.75	6006.25	39.08948	-77.9581
BLAN_003	446	446	39.079499	-77.962386
BLAN_006	446	446	39.084621	-77.962278
BLAN_009	5116.57143	5381.14286	39.085574	-77.958408
CLBJ_033	817.666667	902.666667	33.379549	-97.620436
CLBJ_037	566	566	33.320829	-97.583125
CLBJ_039	188.666667	1647	33.328603	-97.582408
CLBJ_040	849	849	33.378889	-97.64828
CLBJ_041	817.666667	817.666667	33.412252	-97.662234
CLBJ_042	1686.66667	2149.28889	33.371728	-97.596108
CLBJ_057	566	566	33.374409	-97.642297
CPER_002	0	637.6	40.810459	-104.73087
CPER_004	5165	10342.55	40.813091	-104.69854
CPER_005	205	6237.25	40.854109	-104.72692
CPER_006	0	7280	40.813581	-104.74875
CPER_008	0	7280	40.798781	-104.74749
CPER_009	0	637.6	40.82539	-104.74734
CPER_011	1600.4	7355.82	40.86758	-104.70364
CPER_015	4771.5	10178.3	40.853174	-104.74301

| DCFS_003 | 6743.29167 | 33288.875 | 47.204875 | -99.184072 |
| DCFS_004 | 820 | 1591 | 47.170237 | -99.05172 |

Figure A2. Spatial distribution of estimated demand (g/ha) for fruits and seeds across NEON plots. Top two maps show frugivory and granivory demand by birds; bottom two maps show corresponding demand by small mammals. Demand values were derived from body mass, diet fraction, and detection-based density estimates at each NEON site. Warmer colors indicate higher estimated demand
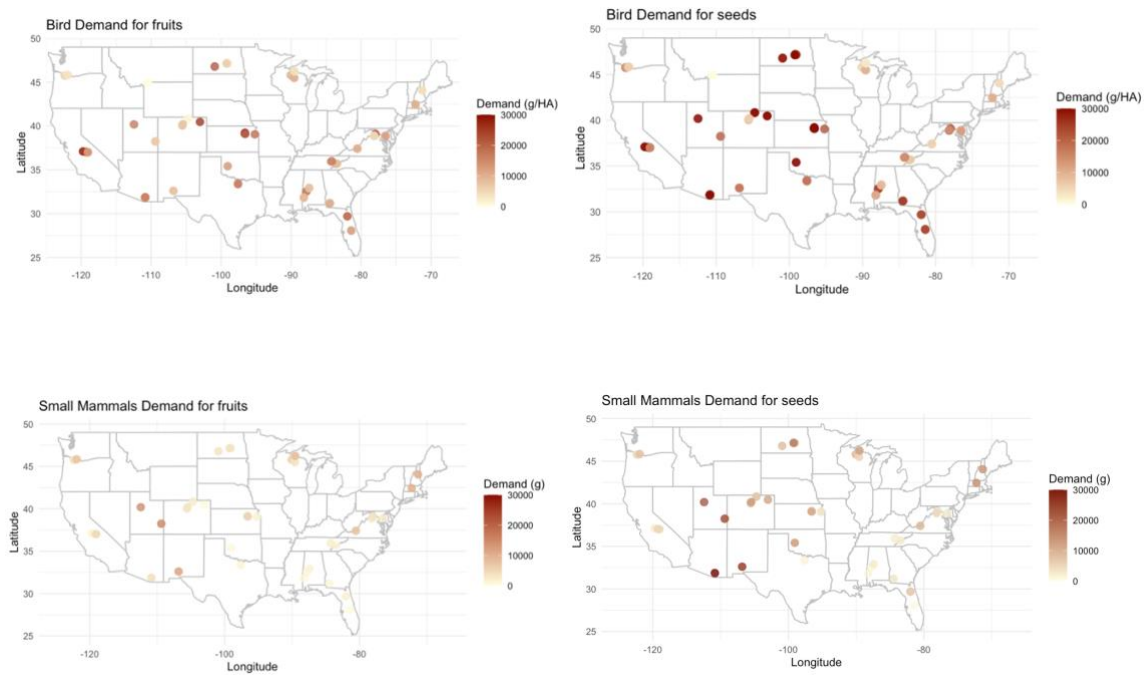

Table A4. Posterior estimates from the Predictive Trait Model (PTM) for zoochory and anemochory. For each dispersal mode, predictor effects are reported as posterior means with standard error (SE) and 95% credible intervals (CI_025, CI_975). Asterisks (*) indicate statistically significant estimates (credible interval excludes zero). Table is sorted by estimate.

Zoochory

trait	Estimate	SE	CI_025	CI_975	sig95
intercept	31.8	9.19	12.8	47.6	*
tpi	0.211	0.123	-0.0174	0.416	
demandHA	6.88E-06	8.72E-05	-0.000141	0.00021	
prec	-0.0879	0.054	-0.184	0.0165	
temp	-0.472	0.391	-1.36	0.289	
WindSpeed	-1.27	1.26	-3.63	1.42	

Anemochory:

trait	Estimate	SE	CI_025	CI_975	sig95
intercept	2.42	8.01	-13.7	16.6	
temp	0.462	0.388	-0.377	1.22	

tpi	0.142	0.11	-0.0785	0.334
WindSpeed	0.00979	0.861	-1.63	1.7
demandHA	7.06E-05	8.46E-05	-5.41E-05	0.000255
prec	-0.0105	0.0582	-0.123	0.0975

Table A5. Species-level wind speed effect estimates from the PTM for anemochorous species. Posterior means, standard errors (SE), and 95% credible intervals (CI_025, CI_975) are reported for each species. Asterisks (*) indicate statistically significant effects. Some ssociated trait values are included here, including seed energy content (kCalPerGm) and maximum plant height (maxHt). Table is sorted by estimate. Only display subset of the table due to space limitation.

species	Estimate	SE	CI_025	CI_975	sig95	kCalPerGm	maxHt
abiesBalsamea	0.0727	0.0145	0.0355	0.0885	*	6.8	18
acerPensylva	0.0589	0.0224	0.00719	0.088	*	4.845	4
acerSpicatum	0.0569	0.0224	0.00256	0.0878	*	4.845	4
betulaAlleghan	0.0569	0.0204	0.00978	0.0871	*	5.25	23
betulaPapyrife	0.0558	0.0233	0.00668	0.0881	*	5.4	21
pinusResinosa	0.0475	0.0252	-0.00316	0.087		6.1	24
thujaPlicata	0.046	0.0272	-0.0145	0.0868		6	50
piceaMariana	0.0446	0.0283	-0.0154	0.0867		6.1	20
tsugaHeteroph	0.0428	0.0257	-0.00798	0.0856		5.7	60
acerSaccharu	0.0407	0.0232	-0.00945	0.0815		4.6	35
piceaRubens	0.0401	0.0266	-0.00969	0.0861		6.475	25.5
fraxinusAmerican	0.0365	0.0244	-0.0133	0.0808		5.2	27
fraxinusNigra	0.0321	0.0211	-0.00708	0.0765		5.2	27
betulaLenta	0.0312	0.0253	-0.019	0.0785		5.25	21
pinusJeffreyi	0.0289	0.0304	-0.0267	0.0844		5.8	38.28461538
abiesAmabilis	0.0272	0.0259	-0.0221	0.0785		6.9	55
pinusContorta	0.0239	0.0297	-0.0309	0.0806		6	30
acerRubrum	0.0238	0.0144	-0.0045	0.0515		4.845	27
tsugaCanadens	0.0231	0.0363	-0.0477	0.0842		5.7	32
pinusStrobus	0.0223	0.0351	-0.045	0.0813		5.551	46
pinusLamberti	0.0197	0.0313	-0.0389	0.0801		6.5	76
piceaEngelman	0.0194	0.0351	-0.0533	0.0838		6.7	25.5
pinusPonderos	0.0156	0.0347	-0.0509	0.0816		5.6	75
liriodenTulipife	0.0147	0.0243	-0.0397	0.0572		0	37

Some portions of the text were refined using ChatGPT (OpenAI, 2024) for grammar and clarity.